Cross-level Attention with Overlapped Windows for Camouflaged Object Detection

Jiepan Li[1#], Fangxiao Lu[1#], Nan Xue[2], Zhuohong Li[1], Hongyan Zhang[1,3], Wei He[1*]
[1]Wuhan University [2]Ant Group [3]China University of Geosciences(Wuhan)
{jiepanli, fangxiaolu, ashelee, zhanghongyan, weihe1990}@whu.edu.cn; xuenan@ieee.org

Abstract

Camouflaged objects adaptively fit their color and texture with the environment, which makes them indistinguishable from the surroundings. Current methods revealed that high-level semantic features can highlight the differences between camouflaged objects and the backgrounds. Consequently, they integrate high-level semantic features with low-level detailed features for accurate camouflaged object detection (COD). Unlike previous designs for multi-level feature fusion, we state that ***enhancing low-level features is more impending for COD****. In this paper, we propose an overlapped window cross-level attention (OWinCA) to achieve the low-level features enhancement guided by the highest-level features. By sliding an aligned window pair on both the highest- and low-level feature maps, the high-level semantics are explicitly integrated into the low-level details via cross-level attention. Additionally, it employs an overlapped window partition strategy to alleviate the incoherence among windows, which prevents the loss of global information. These adoptions enable the proposed OWinCA to enhance low-level features by promoting the separability of camouflaged objects. The associated proposed OWinCANet fuses these enhanced multi-level features by simple convolution operation to achieve the final COD. Experiments conducted on three large-scale COD datasets demonstrate that our OWinCANet significantly surpasses the current state-of-the-art COD methods.*

1. Introduction

Camouflaged objects always adapt their color and texture by employing a background matching strategy [6] to seamlessly blend into complex backgrounds. As illustrated in Fig. 1a, the high similarity between the camouflaged creatures and their backgrounds raises significant challenges for camouflaged object detection (COD). According to existing Fully Convolutional Network (FCN)-based [41] COD methods, high-level features from the encoder contain rich semantic information, which can be used to identify certain degrees of camouflage information. However, although low-level features have a higher resolution and can retain some detailed information [2], they are often difficult to distinguish the camouflaged parts due to insufficient semantic information.

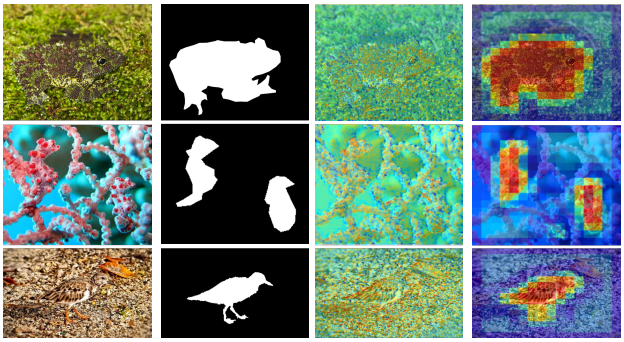

(a) Image (b) Ground Truth (c) low-level features from encoder (d) low-level enhanced features via **OWinCA**

Figure 1. The illustrative visualization of low-level encoded features from PVT-v2 [56] and the enhanced result via our proposed overlapped window cross-level attention (OWinCA).

To solve this problem, state-of-the-art (SOTA) COD decoding strategies focused on the fusion of multi-level encoded features, which generally adopted hierarchical and progressive structures [11, 20, 22, 48] to implicitly fuse high-level semantics with low-level features or introduced boundary supervision [15, 54, 76] to promote the details of the fused features. However, due to the lack of explicit semantic guidance during multi-level feature fusion, the discriminability of camouflaged details is insufficient [17] to fully express the overall information about camouflaged objects. Meanwhile, the representations of the objects and boundaries are frequently inconsistent [30], which may lead to unmatched detection results.

Different from the previous decoder designs for multi-level feature fusion, we claim that explicit guidance from high-level semantics to low-level features can efficiently enhance the representation in camouflaged details. In this

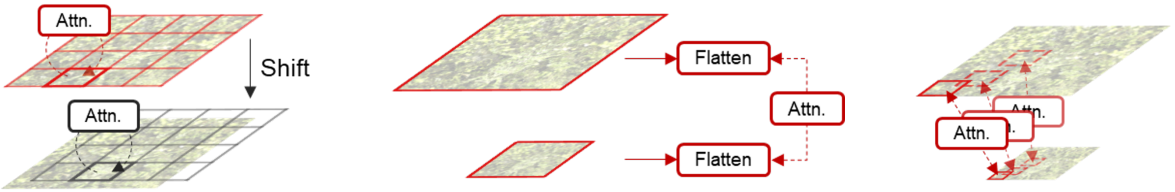

(a) Shifted window self-attention (b) Non-local cross-attention (c) OWinCA (ours)

Figure 2. The explanatory description of the typical structures including (a) shifted window self-attention; (b) non-local cross-attention; and (c) proposed OWinCA. "Attn." represents the typical multi-head attention operation in [8, 38].

paper, we propose an overlapped window cross-level attention (OWinCA) mechanism to enhance low-level features. Specifically, in the OWinCA mechanism, local window pairs are partitioned on multi-level encoded features and continually slide over the entire features with overlapping, where the cross-level window pairs correspond to the same content of the input image (see Fig. 2c). By performing multi-head attention operations between the cross-level window pairs, we can explicitly integrate semantic information from high-level windows into low-level windows, which enhances the discrimination of camouflage objects in the low-level detailed features and avoids excessive independence among windows.

Based on such an efficient low-level feature enhancement strategy, we further introduce a simple OWinCANet, which utilizes the highest-level encoded features to enhance the rest of lower-level encoded features via OWinCA, aligns all the features in the spatial domain, and employs a single convolutional block to yield the final camouflage detection results. As shown in Fig. 1, it is obvious that the lowest-level encoded features can not well distinguish the camouflaged parts (see Fig. 1c). However, by conducting the OWinCA mechanism (see Fig. 1d), the main parts of the camouflaged object become significantly distinguishable. In summary, our contributions include:

- We innovatively introduce an overlapped window cross-level attention (OWinCA) mechanism to explicitly enhance the low-level features with the guidance of the highest-level semantic features.
- We propose a concise and efficient COD network, named OWinCANet, to achieve an outstanding performance over current SOTA COD methods on three large-scale COD datasets.

2. Related Work

2.1. The Designs of Decoders in COD

Based on the encoder-decoder architecture of FCN [41], recent COD approaches explore the designs of efficient decoders for aggregating camouflaged information from multi-level features extracted by multifarious encoder networks like VGG [51], ResNet [16], Res2Net [13], ViT [8], and PVT [55].

In general, commonly used decoders for COD can be categorized into the following types:

1)**Multi-scale-context based approaches** [1, 37, 48, 52, 72, 75]: These approaches develop the multi-scale context modules to describe camouflage objects in different scales and with diverse appearances.

2) **Mechanism-simulation based approaches**: These methods emulate animal hunting processes [10, 11, 42, 46, 65, 67] or human visual detection systems [21, 22, 28, 32, 59], which employ a multi-stage coarse-to-fine strategy to progressively refine detection results.

3) **Boundary-supervision based approaches** [3, 3, 15, 18, 29, 49, 54, 66, 76, 77]: These methods intensify the regularization on the boundary of the camouflage objects, which achieve precise detection outcomes with more obvious texture details.

4) **Frequency-domain integrated approaches** [5, 15, 34, 74]: These involve exploring distinguishable camouflage cues in the frequency domain, which are utilized as the auxiliary information to better investigate camouflage in the spatial domain.

5) **Joint-task based approaches** [23, 27, 63, 71]: These methods integrate salient object detection with COD and extract the common attributes possessed by the two tasks to ultimately achieve a more comprehensive understanding of COD.

6) **Uncertainty-estimation based approaches** [24, 27, 36, 43, 61, 69]: These methods approximate the uncertainty among different areas in the image to guide the model focus on regions hard to be identified, resulting in high-confidence detection.

However, the low-level details extracted by the above-mentioned methods are always of low quality to extract the distinguishable camouflaged details. We state that explicit guidance from high-level semantics is vital for a thorough enhancement of the low-level features, which is urged by high-performance COD methods.

2.2. Window-based Attention

Swin [38] was the first to introduce the shifted windowing strategy, which divides input tokens into non-

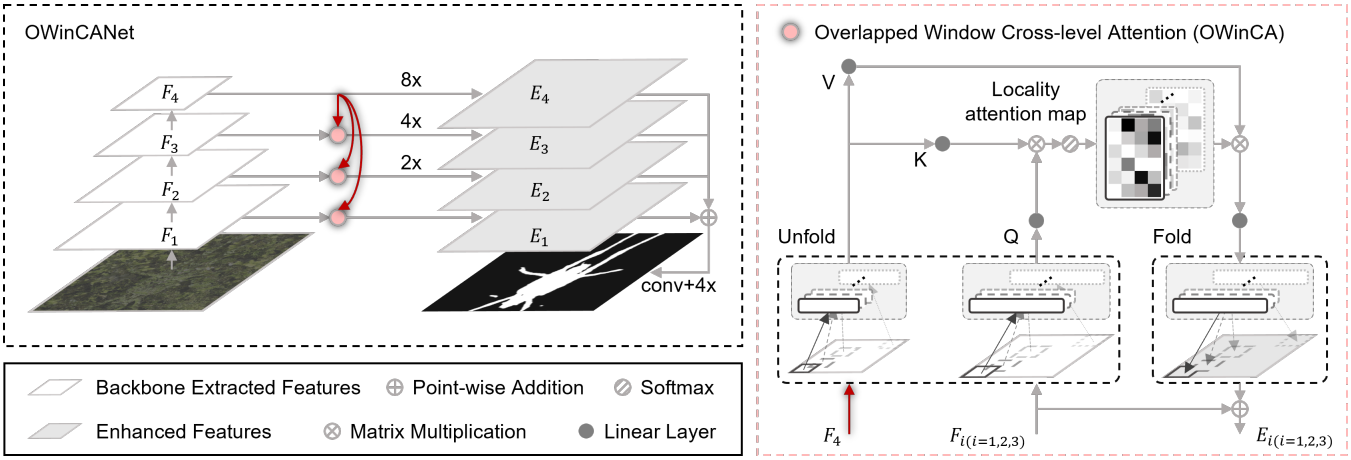

Figure 3. The pipeline of our proposed Overlapped Window Cross-level Attention Network(OWinCANet). The **red arrows** indicate the feature guiding paths from the highest level to low levels. "$n\times$" refers to up-sampling feature maps by a factor of n.

overlapping windows. This approach performed self-attention within each window, achieving a trade-off between model performance and computational efficiency. Inspired by the window-based paradigm, many window-based attention mechanisms based on this strategy have emerged recently [4, 7, 14, 33, 40, 45, 50, 56, 60, 62, 64, 68, 70]. For example, [60] introduced a large window attention that allows the local window to capture the contextual information at multiple scales. [68] proposed the Varied-Size Window Attention (VSA) to learn adaptive window configurations from the input data.

The existing window-based strategies generally adopt independent single-layer self-attention in the encoder layers without consideration of the cross-level information exchange. Additionally, the shifted window partition (see Fig. 2a) ignores the relationships among windows, resulting in the incoherence of the detected results. However, cross-level window-based attention (see Fig. 2c) integrating the high-level semantics into the low-level details is necessary to realize the high separability of the detected camouflaged objects, but is ignored by current methods.

2.3. Multi-level Feature Fusion

Implicit Feature Fusion: Commonly used strategies combine contextual modules with up-sampling operations to construct a feature pyramid network (FPN [35]), progressively merging multi-level features. In FPN, bilinear interpolation inevitably leads to feature misalignment, prompting some studies [17, 19, 31] to learn 2D transformation offsets among features at different levels, which help to achieve a more precise alignment of multi-level features. Meanwhile, Zheng *et al.* [73] introduced a global representation embedding into FPN to realize the low-level feature enhancement.

Explicit Feature Fusion: Tang *et al.* [57] modified the non-local self-attention (see Fig. 2b) to achieve explicit interaction among layers by implementing a cross-level attention mechanism.

However, implicit feature fusion strategies can not supply sufficient high-level semantics, which is essential for the high separability of low-level details in COD. Besides, the prominent discrimination among camouflaged objects is assembled in local regions like edges and textures, which is easily ignored by the non-local attention related explicit feature fusion strategies. Meanwhile, increasing feature resolution leads to exponentially raised computational costs, which is not suitable for efficient COD.

3. Methodology

3.1. Overview

The overall structure of our OWinCANet is illustrated in Fig. 3. We employ a pre-trained Pyramid Vision Transformer (PVT-V2 [55]) network from ImageNet as the encoder to extract four-layer encoded features ($F_i, \{i = 1, 2, 3, 4\}$) regarding the input camouflaged image. Subsequently, we leverage the OWinCA mechanism to sequentially enhance the first three low-level encoded features, F_1, F_2, and F_3, using the highest-level encoded feature, F_4. Then, the four-level features are up-sampled to the same resolution. The enhanced multi-level features, represented by:

$$E_i = \begin{cases} U_i(OWinCA_i(F_4, F_i)), & i = 1, 2, 3 \\ U_i(F_4), & i = 4, \end{cases} \quad (1)$$

where U_i refers to the up-sampling operation with scale factor of 2^{i-1}.

Finally, the enhanced multi-level features are fused together by simple addition, and the camouflage detection result C_{out} is directly output through a classifier that consists

of a convolutional layer sequence, which is given as:

$$C_{out} = Classifier(\sum_{i=1}^{4} E_i). \quad (2)$$

3.2. Overlapped Window Cross-level Attention

In the design of our OWinCA, we grasp two key points: **(1)** the subtle differences between camouflaged objects and the complex background are mainly reflected on local scales; **(2)** explicit guidance derived from high-level semantics can be conveyed to low-level details at the corresponding positions.

As shown in Fig. 3, given two input features, $F_4 \in R^{B\times C\times H_4\times W_4}$ from the highest-level and $F_i \in R^{B\times C\times H_i\times W_i}$ from the low-level, where B, C, $H_{i/4}$, and $W_{i/4}$ denote batch size, number of channels, height, and width, respectively, we first compute the scale factor S_s for the two features in the spatial domain, which can be written as:

$$S_s = \frac{H_i}{H_4}. \quad (3)$$

Subsequently, We introduce an overlapped window unfolding strategy to partition local window pairs with matched image content on multi-level encoded features and continually slide them over the entire feature map with a certain degree of overlapping. In detail, for high-level features, we set the window size to be k with an overlapping of $\frac{k}{2}$. Correspondingly, for low-level features, the sizes of both window and overlapping are S_s times the ones of the high-level features. Then, we can obtain m feature pairs from high- and low-level local windows, where $m = \frac{H_4-k}{k/2} + 1$.

Then the unfolded feature pairs are processed by a sequence of operations, including reshaping, transposing, flattening, and layer normalization to get the corresponding tensors $T_i \in R^{B^{'}\times(S_s\cdot k)^2\times C}$ and $T_4 \in R^{B^{'}\times(k)^2\times C}$, where $B^{'} = B \cdot m$.

Immediately, we perform a linear transformation and multi-heads decomposition on both T_4 and T_i, and we can get the corresponding query tensor q, key tensor k, and value tensor v, which can be represented by:

$$\begin{aligned} q &= Transpose(MH(Linear(T_i))), \\ q &\in R^{B^{'}\times Heads\times(S_s\cdot k)^2\times\frac{C}{Heads}}, \end{aligned} \quad (4)$$

$$\begin{aligned} k &= Transpose(MH(Linear(T_4))), \\ k &\in R^{B^{'}\times Heads\times k^2\times\frac{C}{Heads}}, \end{aligned} \quad (5)$$

$$\begin{aligned} v &= Transpose(MH(Linear(T_4))), \\ v &\in R^{B^{'}\times Heads\times k^2\times\frac{C}{Heads}}, \end{aligned} \quad (6)$$

where MH means the multi-head decomposition. Subsequently, we conduct the multi-head self-attention to calculate the similarity of each head as below:

$$O_i = Attention(q,k,v) = Softmax(\frac{qk^T}{\sqrt{d}})v, \quad (7)$$

where $d = \frac{C}{Heads}$.

With that, the output tensor O_i is transposed, flattened, and transformed with a linear layer. Then, the folding strategy is adopted to restore O_i to the original shape as F_i. Finally, in order to maintain the original low-level information, a residual structure is introduced with a learnable weight α, so the final enhanced features E_i can be defined as:

$$E_i = \alpha \cdot O_i + (1-\alpha)\cdot F_i. \quad (8)$$

Owing to the explicit semantic guidance from high level to low level, the E_i not only possesses semantic information but also preserves sufficient detailed information.

3.3. Loss Function

As shown in Fig.3, our OWinCANet just outputs a final camouflage detection result C_{out}, which can be used to build the loss function with the ground truth (GT). Weighted binary cross-entropy ($wbce$) loss and weighted intersection over union ($wiou$) loss are used to construct the loss function[58]. Therefore, the total loss function $loss$ can be described as:

$$loss = loss_{wbce}(C_{out}, GT) + loss_{wiou}(C_{out}, GT). \quad (9)$$

4. Experiment

4.1. Datasets

Three datasets were used to evaluate the proposed model: CAMO [26], COD10K [10], and NC4K[42]. These three datasets differ significantly. NC4K is the largest dataset, which contains 4,121 images downloaded from the website. COD10K includes 78 camouflaged categories, with 3,040 training images and 2,026 test images in total. CAMO provides 1,250 images in total, including eight categories with 1,000 training images and 250 test images. According to [11], we used the training images from the CAMO and COD10K datasets as the training set (4,040 images) and the test images from CAMO [26], COD10K [10], and NC4K[42] as the test set.

4.2. Evaluation Metrics

Following the previous work [11, 15, 48], we selected the structure-measure (S_α) [9], E-measure (E_ϕ) [12], weighted F-measure (F_β^w) [44] and mean absolute error (M) as the evaluation metrics.

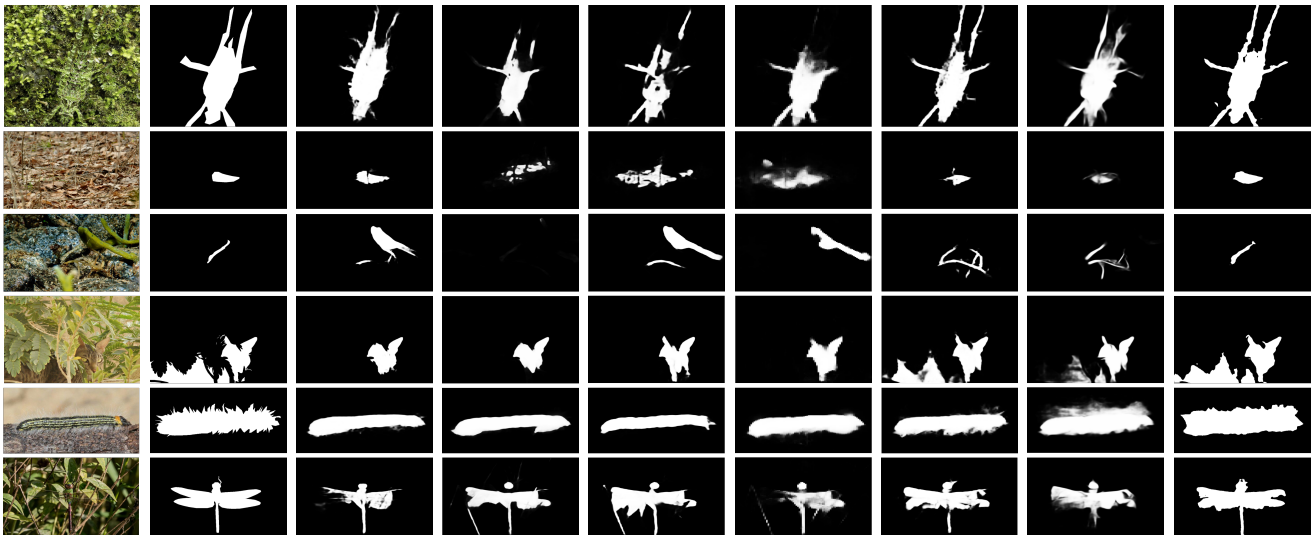

(a) Image (b) GT (c) SegMaR (d) ZoomNet (e) FEDER (f) FDNet (g) UEDG (h) FSPNet (i) **Ours**

Figure 4. Visual comparison between our OWinCANet with other SOTA methods.

Table 1. Performance comparison with baseline models on COD datasets. ↑ indicates the higher the score the better and vice versa. The best score for each metric is highlighted in bold.

Baseline	CAMO (250 images)				COD10K (2026 images)				NC4K (4121 images)			
	$S_\alpha \uparrow$	$E_\phi \uparrow$	$F_\beta^w \uparrow$	$M \downarrow$	$S_\alpha \uparrow$	$E_\phi \uparrow$	$F_\beta^w \uparrow$	$M \downarrow$	$S_\alpha \uparrow$	$E_\phi \uparrow$	$F_\beta^w \uparrow$	$M \downarrow$
SINet v2 [11]$_{TPAMI2022}$	0.820	0.882	0.743	0.070	0.815	0.887	0.680	0.037	0.847	0.903	0.767	0.048
ZoomNet [48]$_{CVPR2022}$	0.820	0.892	0.752	0.066	0.838	0.911	0.729	0.029	0.853	0.912	0.784	0.043
SegMaR [22]$_{CVPR2022}$	0.815	0.872	0.742	0.071	0.833	0.895	0.724	0.033	0.841	0.907	0.781	0.046
BGS-Net [76]$_{AAAI2022}$	0.796	0.851	0.717	0.079	0.818	0.891	0.699	0.034	0.814	0.897	0.771	0.048
FAP-Net [75]$_{TIP2022}$	0.815	0.865	0.776	0.076	0.822	0.731	0.888	0.036	0.851	0.901	0.775	0.047
FindNet [29]$_{TIP2022}$	0.800	0.862	0.725	0.077	0.811	0.883	0.688	0.036	0.841	0.895	0.769	0.048
BGNet [54]$_{IJCAI2022}$	0.812	0.870	0.749	0.073	0.831	0.901	0.722	0.033	0.851	0.907	0.788	0.044
UR-SINet v2 [24]$_{ACM2022}$	0.814	0.891	0.758	0.067	0.816	0.903	0.708	0.033	0.844	0.910	0.787	0.045
FDNet [74]$_{CVPR2022}$	0.842	0.895	0.774	0.063	0.837	0.918	0.731	0.030	0.834	0.893	0.750	0.052
DTIT[39]$_{ICPR2022}$	0.857	0.916	0.796	0.050	0.824	0.896	0.695	0.034	0.863	0.917	0.792	0.041
HitNet[18]$_{AAAI2023}$	0.844	0.902	0.801	0.057	0.868	0.932	0.798	0.024	0.870	0.921	0.825	0.039
FEDER [15]$_{CVPR2023}$	0.836	0.897	0.807	0.066	0.844	0.911	0.748	0.029	0.862	0.913	0.824	0.042
EAMNet [53]$_{ICME2023}$	0.831	0.890	0.763	0.064	0.839	0.907	0.733	0.029	0.862	0.916	0.801	0.040
PENet [32]$_{IJCAI2023}$	0.828	0.890	0.771	0.063	0.831	0.908	0.723	0.031	0.855	0.912	0.795	0.042
UEDG [43]$_{TMM2023}$	0.868	0.922	0.819	0.048	0.858	0.924	0.766	0.025	0.881	0.928	0.829	0.035
FPNet [5]$_{MM2023}$	0.852	0.905	0.806	0.056	0.850	0.913	0.748	0.029	-	-	-	-
FSPNet [20]$_{CVPR2023}$	0.856	0.899	0.799	0.050	0.851	0.895	0.735	0.026	0.879	0.915	0.816	0.035
OPNet [47]$_{IJCV2023}$	0.858	0.915	0.817	0.050	0.857	0.919	0.767	0.026	0.883	0.932	0.838	0.034
Ours	**0.879**	**0.946**	**0.860**	**0.038**	**0.875**	**0.947**	**0.818**	**0.019**	**0.889**	**0.947**	**0.864**	**0.028**

4.3. Implementation detail

All experiments were conducted using PyTorch 2.0.1 on an NVIDIA GeForce RTX 3090 GPU with 24 GB memory. During training, the batch size was set to 8, the input images were all resized to 512×512, and the Adam [25] optimizer was employed. For all experiments, the models were trained for 40 epochs with a poly learning rate policy, where the initial learning rate was set to 0.0001 and multiplied by $(1 - \frac{epoch}{max\_epoch})^{power}$, where $power = 0.9$. Besides, horizontal flips, vertical flips, and the mosaic strategy were adopted for data augmentation.

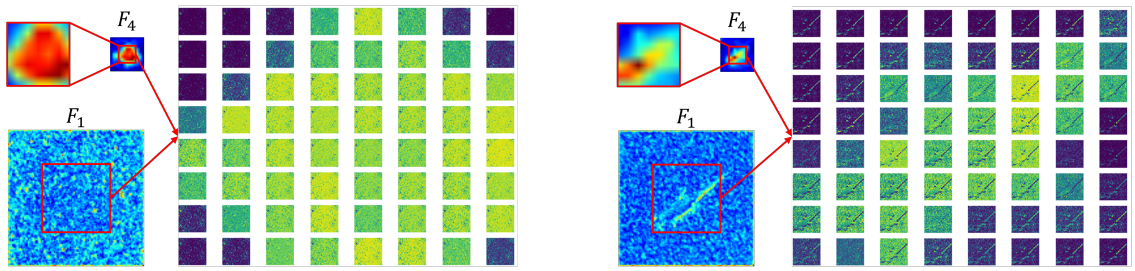

(a) Example 1 (b) Example 2

Figure 5. Visualization of the locality attention map inside OWinCA. The window size of F_4 and F_1 is 8×8 and 64×64, respectively.

4.4. Compared Methods

In order to evaluate the superiority of the proposed model on the COD task, we selected several SOTA methods for comparison: *i.e.*, **CNN-based**: SINet v2 [11], ZoomNet [48], SegMaR [22], BGS-Net [76], FAP-Net [75], FindNet [29], BGNet [54], UR-SINet v2 [24], FDNet [74], FEDER [15], and PENet [32]; **Transformer-based**: DTIT [39], HitNet [18], EAMNet [53], UEDG [43], FPNet [5], FSPNet [20], and OPNet [47].

4.5. Visual Analysis

Fig. 4 demonstrates the qualitative comparison of our OWinCA with other SOTA camouflage object detection (COD) methods. It is evident that existing methods struggle to accurately detect objects in highly camouflaged scenarios, resulting in false positives and omissive detections (2nd and 3rd images). Furthermore, when camouflaged objects are partially occluded by the background and appear with discontinuous appearance, existing methods often struggle to capture the global context of the objects (4th and 6th images). Additionally, existing methods perform inadequate detection of camouflaged objects with irregular and complex edges (1st and 5th images). By contrast, our method achieves high-precision detection results in handling diverse scenarios with complex structures. This phenomenon strongly indicates the effectiveness of our OWinCA mechanism, which enables fine-grained manipulation of camouflage details and an overall estimation of the spatial structural information of the camouflaged objects.

4.6. Quantitative Evaluation

To further demonstrate the superiority of our method, we conducted a comprehensive quantitative evaluation and compared it to existing SOTA COD methods. The results, as shown in Tab. 1, strongly demonstrate the dominant position of our method, which surpass other methods over all metrics. Specifically, on the CAMO dataset, our OWinCANet exhibits significant improvements over the SOTA method UEDG [43], with a 1.1% increase in S_α, a 2.4% increase in E_ϕ, and a 4.1% increase in F_β^w. Additionally, our method achieves a 1% reduction in M, where smaller M denotes better performance. On the COD10K dataset, OWinCANet outperforms OPNet [47] by 1.8%, 2.8%, 5.1%, and 0.7% in terms of S_α, E_ϕ, F_β^w, and M, respectively. Moreover, on the larger NC4K dataset, our OWinCANet also achieves a remarkable lead over the corresponding SOTA method OPNet [47], improving S_α, E_ϕ, and F_β^w by 0.6%, 1.5%, and 2.6%, while reducing M by 0.6%. These concrete quantitative comparisons highlight the effectiveness of the proposed explicit semantic guidance approach and firmly establish the superiority of our method in addressing the challenging problems faced by the camouflage detection.

Table 2. Comparison of with/without OWinCA.

Baseline	COD10K (2026 images)				NC4K (4121 images)			
	$S_\alpha \uparrow$	$E_\phi \uparrow$	$F_\beta^w \uparrow$	$M \downarrow$	$S_\alpha \uparrow$	$E_\phi \uparrow$	$F_\beta^w \uparrow$	$M \downarrow$
w/o OWinCA	0.805	0.875	0.663	0.038	0.837	0.891	0.754	0.050
OWinCA	**0.875**	**0.947**	**0.818**	**0.019**	**0.889**	**0.947**	**0.864**	**0.028**

5. Discussion

In order to further validate the effectiveness of our method, particularly the advantages derived from the operations performed within the overlapped window cross-level attention (OWinCA) for camouflage object detection (COD), we conducted a comprehensive set of ablation experiments. In this section, we will present a detailed explanation and analysis.

5.1. The Effectiveness of OWinCA

With/Without OWinCA: Firstly, we evaluated the impact of the OWinCA module, a plug-and-play component with a special design for accurate COD task. Without OWinCA, all feature layers were directly up-sampled and fused together after being extracted from the backbone network, to generate the camouflage detection results. The results, as shown in Tab. 2, clearly demonstrate that incorporating OWinCA leads to a significant improvement in the overall performance, with substantial gains over the four evaluation metrics on the test datasets.

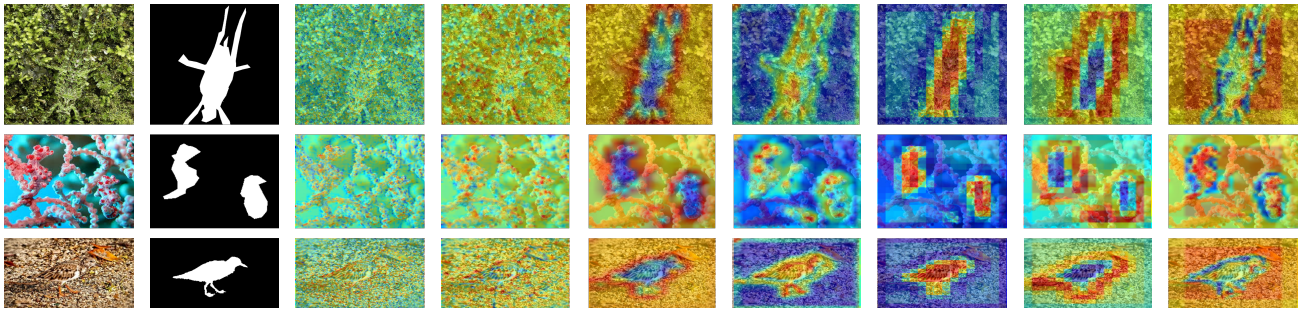

(a) Image (b) GT (c) F_1 (d) F_2 (e) F_3 (f) F_4 (g) E_3 (h) E_2 (i) E_1

Figure 6. Visualization of encoded features F_i and enhanced features E_i via proposed OWinCA.

Table 3. Comparison of different window sizes.

$\{k_1, k_2, k_3\}$	COD10K (2026 images)				NC4K (4121 images)			
	$S_\alpha \uparrow$	$E_\phi \uparrow$	$F_\beta^w \uparrow$	$M \downarrow$	$S_\alpha \uparrow$	$E_\phi \uparrow$	$F_\beta^w \uparrow$	$M \downarrow$
$\{2, 2, 2\}$	0.856	0.936	0.785	0.023	0.876	0.939	0.844	0.032
$\{4, 4, 4\}$	0.860	0.940	0.793	0.022	0.881	0.942	0.850	0.030
$\{6, 6, 6\}$	0.859	0.937	0.790	0.022	0.880	0.942	0.850	0.031
$\{8, 8, 8\}$	0.870	0.944	0.808	0.020	0.886	0.944	0.857	0.029
$\{16, 16, 16\}$	0.849	0.921	0.765	0.026	0.858	0.923	0.831	0.034
$\{8, 4, 2\}$	**0.875**	**0.947**	**0.818**	**0.019**	**0.889**	**0.947**	**0.864**	**0.028**

Locality Attention Map in OWinCA: To clearly illustrate the advantages of the OWinCA mechanism, we have carefully selected two examples (Fig. 5a,5b) to further demonstrate the enhancement of E_1 brought by the module. As shown in Fig. 5, we have visualized the locality attention map constructed between the partitioned windows marked by red boxes. The window sizes of the illustrated features are 8×8 and 64×64, respectively. Correspondingly, the overall attention map on the right side of each example consists of 8×8 attention sub-maps with sizes of 64×64. These sub-maps represent the correlation between each pixel in the highest-level feature window and all pixels of the low-level feature window. Moreover, the 8×8 sub-map array exhibits the same attention pattern as the highest-level feature window, which demonstrates the effectiveness of our proposed mechanism in semantically embedding foreground and background in low-level features. It is evident that this cross-level attention mechanism, based on the overlapped window partition strategy, effectively integrates the semantic information from the high-level features into the corresponding details represented by the low-level features, enabling precise expression of camouflage objects.

Visual Comparison before/after OWinCA: Meanwhile, we qualitatively compared the vanilla features F_1, F_2, F_3 with the enhanced features E_1, E_2, E_3. From Fig. 6, it is visible that, positively affected by the OWinCA, the expression of camouflage information in each feature layer is greatly enhanced, and the overall structure of the camouflage becomes more obvious and discernible.

Window Sizes in OWinCA: To evaluate the influence of local window size in the cross-level attention mechanism proposed in this paper, we conducted experiments using five sets of window sizes: $\{k_1, k_2, k_3\}$=$\{2, 2, 2\}$, $\{4, 4, 4\}$,$\{6, 6, 6\}$,$\{8, 8, 8\}$,$\{16, 16, 16\}$,$\{8, 4, 2\}$, where i corresponds to the guided i_{th} layer with the highest-level encoded features. The results are presented in Tab. 3. Considering that the input image size being 512×512, the spatial size of F_4 is only 16×16. Therefore, when the window size is 16, it implies that there is no window partition and non-local attention is conducted on the features. From Tab. 3, we can easily observe that, compared with the non-local attention, our overlapped window partition strategy brings much higher improvements on the detection results. Furthermore, compared to the constant window size, an adaptive window size accommodating with the spatial size of the relevant feature map allows for a flexible local region to be processed, contributing to a superior detection performance with more matching camouflaged detail capturing. Consequently, we selected $\{k_1, k_2, k_3\}$=$\{8, 4, 2\}$, which ensures the best performance while keeping computational overhead manageable.

5.2. The Effectiveness of Overlapping Strategy

With/Without Overlapping: To validate the effectiveness of the overlapped local windows employed in the cross-level attention mechanism, we conducted a comprehensive comparison from both quantitative and qualitative perspectives. In the quantitative evaluation, we compared experiments with or without overlapping in the window partition process. As shown in Tab. 4, it's evident that using overlapped windows contributes to a significant improvement in accuracy. For the qualitative analysis, as depicted in Fig. 7, we visualized the lowest-level features processed by the two methods under comparison. It is apparent that the lack of overlap between windows leads to incoherence in the detection results. Even though lowest-level features are enhanced to some extent in this case, the loss of internal object information is inevitable due to the disconnections among partitioned windows. These observations further emphasize the importance of overlapped window adoption.

Table 4. Comparison of different cross-level attention strategies under different window partition settings.

Baseline	COD10K (2026 images)				NC4K (4121 images)			
	$S_\alpha \uparrow$	$E_\phi \uparrow$	$F_\beta^w \uparrow$	$M \downarrow$	$S_\alpha \uparrow$	$E_\phi \uparrow$	$F_\beta^w \uparrow$	$M \downarrow$
Non-local	0.849	0.921	0.765	0.026	0.858	0.923	0.831	0.034
Shifted	0.848	0.930	0.773	0.025	0.868	0.932	0.832	0.035
Non-overlap	0.851	0.928	0.777	0.025	0.874	0.934	0.837	0.032
Overlapped	**0.875**	**0.947**	**0.818**	**0.019**	**0.889**	**0.947**	**0.864**	**0.028**

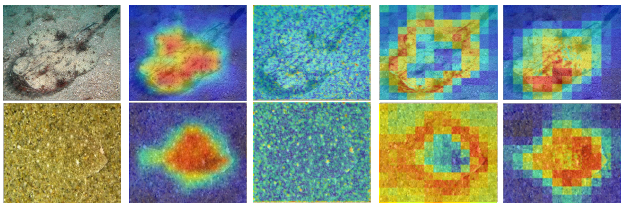

(a) Image (b) F_4 (c) F_1 (d) E_1 via Non-overlap windows (e) E_1 via Overlapped windows

Figure 7. Visual comparison using OWinCA modules with and without overlapping. (b) and (c) is the highest and lowest encoded features output from the pre-trained PVT-V2 [55], respectively. (d) and (e) correspond to the usage of overlapping and non-overlapping strategies in OWinCA, respectively.

Comparison with other Cross-level Attention: Furthermore, to validate the superiority of our proposed OWinCA mechanism, we compared it with the cross-level attention of Non-local, and the shifted window cross-attention improved from shifted window self-attention (see Fig. 2a). The experimental results of the comparison are presented in Tab. 4, where we can observe that our method achieves the most outstanding results compared to the two alternative forms.

Computational Complexity Analysis: Finally, we discussed the computational cost of our OWinCA compared to the non-local cross-level attention. Assuming the image size is $N \times N$, the window size is $k \times k$, and the overlap is $\frac{k}{2}$, we can calculate that the number of obtained windows is $\frac{N-k}{k/2} + 1$. Ignoring the computational cost of the linear layer, the computational cost of OWinCA when the window size is $k \times k$ is $2 \cdot (S_s)^2 \cdot k^4 \cdot \frac{C}{Head} \cdot (\frac{N-k}{k/2} + 1)^2$, while the computational cost of the non-local cross-level attention is $2 \cdot (S_s)^2 \cdot N^4 \cdot \frac{C}{Head}$. It is evident that our OWinCA has a significant advantage in computational cost.

5.3. The Guidance Strategies in Enhancement

The principle of the proposed OWinCA is to use higher-level features as guidance to enhance the lower-level features. In this paper, we chose the highest-level features to enhance the lower-level features separately. However, the third layer features can also guide the enhancement of lower-level features. Following [73], we presented the comparative experimental results of different guidance strategies in Tab. 5. Specifically, we selected semantic information from either the fourth layer or the third layer as guidance, following the principle of common adoption [73]. Tab. 5 gives the results of the comparative experiments in detail. The data presented in Tab. 5 reveals that the semantic guidance from the third-layer feature generates an inferior performance than the one yielded by the fourth-layer semantic guidance. Moreover, the more feature layers processed, the higher improvements in the overall model performance. It eloquently highlights the critical role played by different feature layers in achieving precise detection of camouflaged objects. Meanwhile, we also adopted a progressive guidance structure similar to FPN [35] ($4 \rightarrow 3 \rightarrow 2 \rightarrow 1$). However, the experimental results in Tab. 5 indicate that the results obtained by this guidance method are still inferior to the experimental results obtained by guiding low-level encoding features with the highest-level encoding features, which illustrates the importance of rich high-level semantics for low-level feature implementation of camouflage object distinguishability.

Table 5. Comparison of different guidance strategies.

Strategies	COD10K (2026 images)				NC4K (4121 images)			
	$S_\alpha \uparrow$	$E_\phi \uparrow$	$F_\beta^w \uparrow$	$M \downarrow$	$S_\alpha \uparrow$	$E_\phi \uparrow$	$F_\beta^w \uparrow$	$M \downarrow$
$3 \rightarrow 1$	0.848	0.930	0.773	0.025	0.868	0.932	0.832	0.035
$3 \rightarrow 2$	0.850	0.932	0.776	0.024	0.872	0.934	0.835	0.033
$3 \rightarrow 1, 2$	0.851	0.931	0.777	0.024	0.872	0.935	0.835	0.033
$4 \rightarrow 1$	0.853	0.937	0.781	0.023	0.874	0.939	0.840	0.032
$4 \rightarrow 2$	0.856	0.938	0.786	0.023	0.877	0.940	0.844	0.032
$4 \rightarrow 3$	0.849	0.935	0.776	0.025	0.871	0.937	0.838	0.033
$4 \rightarrow 1, 2$	0.856	0.935	0.784	0.023	0.876	0.938	0.841	0.032
$4 \rightarrow 1, 3$	0.858	0.940	0.789	0.022	0.878	0.941	0.845	0.031
$4 \rightarrow 2, 3$	0.858	0.937	0.789	0.023	**0.890**	0.942	0.848	0.031
$4 \rightarrow 3 \rightarrow 2 \rightarrow 1$	0.866	0.942	0.804	0.021	0.883	0.941	0.853	0.030
$4 \rightarrow 1, 2, 3$	**0.875**	**0.947**	**0.818**	**0.019**	0.889	**0.947**	**0.864**	**0.028**

6. Conclusion

In this paper, we address the inseparable problem of camouflage details (edge, texture, *etc.*), which is caused by insufficient semantic guidance. In detail, we propose a heuristic attention mechanism based on cross-level overlapped window pairs to explicitly convey the semantic information in the highest-level encoded features to the rest of the low-level encoded features, achieving high separability of camouflage information on multi-level features. At the same time, we propose an extremely simple but effective OWinCANet based on the OWinCA mechanism. In addition, we carry out sufficient experiments to verify and analyze the effectiveness of the modules in the ablation experiments, as well as the internal parameter design of the modules and the overall network structure design. We also believe that such an overlapped window cross-level attention mechanism should not only play a role in camouflage object detection task, but also expand this idea to more extensive tasks in future work.

References

[1] Geng Chen, Si-Jie Liu, Yu-Jia Sun, Ge-Peng Ji, Ya-Feng Wu, and Tao Zhou. Camouflaged object detection via context-aware cross-level fusion. *IEEE Transactions on Circuits and Systems for Video Technology*, 32(10):6981–6993, 2022. 2

[2] Liang-Chieh Chen, Yukun Zhu, George Papandreou, Florian Schroff, and Hartwig Adam. Encoder-decoder with atrous separable convolution for semantic image segmentation. In *Proceedings of the European conference on computer vision (ECCV)*, pages 801–818, 2018. 1

[3] Tianyou Chen, Jin Xiao, Xiaoguang Hu, Guofeng Zhang, and Shaojie Wang. Boundary-guided network for camouflaged object detection. *Knowledge-Based Systems*, 248: 108901, 2022. 2

[4] Xiangyu Chen, Xintao Wang, Jiantao Zhou, Yu Qiao, and Chao Dong. Activating more pixels in image super-resolution transformer. In *Proceedings of the IEEE/CVF Conference on Computer Vision and Pattern Recognition*, pages 22367–22377, 2023. 3

[5] Runmin Cong, Mengyao Sun, Sanyi Zhang, Xiaofei Zhou, Wei Zhang, and Yao Zhao. Frequency perception network for camouflaged object detection. *arXiv preprint arXiv:2308.08924*, 2023. 2, 5, 6

[6] Innes C Cuthill, Martin Stevens, Jenna Sheppard, Tracey Maddocks, C Alejandro Párraga, and Tom S Troscianko. Disruptive coloration and background pattern matching. *Nature*, 434(7029):72–74, 2005. 1

[7] Xiaoyi Dong, Jianmin Bao, Dongdong Chen, Weiming Zhang, Nenghai Yu, Lu Yuan, Dong Chen, and Baining Guo. Cswin transformer: A general vision transformer backbone with cross-shaped windows. In *Proceedings of the IEEE/CVF Conference on Computer Vision and Pattern Recognition*, pages 12124–12134, 2022. 3

[8] Alexey Dosovitskiy, Lucas Beyer, Alexander Kolesnikov, Dirk Weissenborn, Xiaohua Zhai, Thomas Unterthiner, Mostafa Dehghani, Matthias Minderer, Georg Heigold, Sylvain Gelly, et al. An image is worth 16x16 words: Transformers for image recognition at scale. *arXiv preprint arXiv:2010.11929*, 2020. 2

[9] Deng-Ping Fan, Ming-Ming Cheng, Yun Liu, Tao Li, and Ali Borji. Structure-measure: A new way to evaluate foreground maps. In *ICCV*, pages 4548–4557, 2017. 4

[10] Deng-Ping Fan, Ge-Peng Ji, Guolei Sun, Ming-Ming Cheng, Jianbing Shen, and Ling Shao. Camouflaged object detection. In *Proceedings of the IEEE/CVF conference on computer vision and pattern recognition*, pages 2777–2787, 2020. 2, 4

[11] Deng-Ping Fan, Ge-Peng Ji, Ming-Ming Cheng, and Ling Shao. Concealed object detection. *IEEE Transactions on Pattern Analysis and Machine Intelligence*, 2021. 1, 2, 4, 5, 6

[12] Deng-Ping Fan, Ge-Peng Ji, Xuebin Qin, and Ming-Ming Cheng. Cognitive vision inspired object segmentation metric and loss function. *SCIENTIA SINICA Informationis*, 6, 2021. 4

[13] Shang-Hua Gao, Ming-Ming Cheng, Kai Zhao, Xin-Yu Zhang, Ming-Hsuan Yang, and Philip Torr. Res2net: A new multi-scale backbone architecture. *IEEE transactions on pattern analysis and machine intelligence*, 43(2):652–662, 2019. 2

[14] Ali Hassani, Steven Walton, Jiachen Li, Shen Li, and Humphrey Shi. Neighborhood attention transformer. In *Proceedings of the IEEE/CVF Conference on Computer Vision and Pattern Recognition*, pages 6185–6194, 2023. 3

[15] Chunming He, Kai Li, Yachao Zhang, Longxiang Tang, Yulun Zhang, Zhenhua Guo, and Xiu Li. Camouflaged object detection with feature decomposition and edge reconstruction. In *Proceedings of the IEEE/CVF Conference on Computer Vision and Pattern Recognition*, pages 22046–22055, 2023. 1, 2, 4, 5, 6

[16] Kaiming He, Xiangyu Zhang, Shaoqing Ren, and Jian Sun. Deep residual learning for image recognition. In *Proceedings of the IEEE conference on computer vision and pattern recognition*, pages 770–778, 2016. 2

[17] Hanzhe Hu, Yinbo Chen, Jiarui Xu, Shubhankar Borse, Hong Cai, Fatih Porikli, and Xiaolong Wang. Learning implicit feature alignment function for semantic segmentation. In *European Conference on Computer Vision*, pages 487–505. Springer, 2022. 1, 3

[18] Xiaobin Hu, Deng-Ping Fan, Xuebin Qin, Hang Dai, Wenqi Ren, Ying Tai, Chengjie Wang, and Ling Shao. High-resolution iterative feedback network for camouflaged object detection. *arXiv preprint arXiv:2203.11624*, 2022. 2, 5, 6

[19] Zilong Huang, Yunchao Wei, Xinggang Wang, Wenyu Liu, Thomas S Huang, and Humphrey Shi. Alignseg: Feature-aligned segmentation networks. *IEEE Transactions on Pattern Analysis and Machine Intelligence*, 44(1):550–557, 2021. 3

[20] Zhou Huang, Hang Dai, Tian-Zhu Xiang, Shuo Wang, Huai-Xin Chen, Jie Qin, and Huan Xiong. Feature shrinkage pyramid for camouflaged object detection with transformers. In *Proceedings of the IEEE/CVF Conference on Computer Vision and Pattern Recognition*, pages 5557–5566, 2023. 1, 5, 6

[21] Ge-Peng Ji, Lei Zhu, Mingchen Zhuge, and Keren Fu. Fast camouflaged object detection via edge-based reversible recalibration network. *Pattern Recognition*, 123:108414, 2022. 2

[22] Qi Jia, Shuilian Yao, Yu Liu, Xin Fan, Risheng Liu, and Zhongxuan Luo. Segment, magnify and reiterate: Detecting camouflaged objects the hard way. In *Proceedings of the IEEE/CVF Conference on Computer Vision and Pattern Recognition*, pages 4713–4722, 2022. 1, 2, 5, 6

[23] Xinhao Jiang, Wei Cai, Yao Ding, Xin Wang, Danfeng Hong, Zhiyong Yang, and Weijie Gao. Camouflaged object segmentation based on joint salient object for contrastive learning. *IEEE Transactions on Instrumentation and Measurement*, 2023. 2

[24] Nobukatsu Kajiura, Hong Liu, and Shin'ichi Satoh. Improving camouflaged object detection with the uncertainty of pseudo-edge labels. In *ACM Multimedia Asia*, pages 1–7. 2021. 2, 5, 6

[25] Diederik P Kingma and Jimmy Ba. Adam: A method for stochastic optimization. *arXiv preprint arXiv:1412.6980*, 2014. 5

[26] Trung-Nghia Le, Tam V Nguyen, Zhongliang Nie, Minh-Triet Tran, and Akihiro Sugimoto. Anabranch network for camouflaged object segmentation. *CVIU*, 184:45–56, 2019. 4

[27] Aixuan Li, Jing Zhang, Yunqiu Lv, Bowen Liu, Tong Zhang, and Yuchao Dai. Uncertainty-aware joint salient object and camouflaged object detection. In *Proceedings of the IEEE/CVF Conference on Computer Vision and Pattern Recognition*, pages 10071–10081, 2021. 2

[28] Jiepan Li, Wei He, and Hongyan Zhang. Towards complex backgrounds: A unified difference-aware decoder for binary segmentation. *arXiv preprint arXiv:2210.15156*, 2022. 2

[29] Peng Li, Xuefeng Yan, Hongwei Zhu, Mingqiang Wei, Xiao-Ping Zhang, and Jing Qin. Findnet: Can you find me? boundary-and-texture enhancement network for camouflaged object detection. *IEEE Transactions on Image Processing*, 31:6396–6411, 2022. 2, 5, 6

[30] Xiangtai Li, Xia Li, Li Zhang, Guangliang Cheng, Jianping Shi, Zhouchen Lin, Shaohua Tan, and Yunhai Tong. Improving semantic segmentation via decoupled body and edge supervision. In *Computer Vision–ECCV 2020: 16th European Conference, Glasgow, UK, August 23–28, 2020, Proceedings, Part XVII 16*, pages 435–452. Springer, 2020. 1

[31] Xiangtai Li, Ansheng You, Zhen Zhu, Houlong Zhao, Maoke Yang, Kuiyuan Yang, Shaohua Tan, and Yunhai Tong. Semantic flow for fast and accurate scene parsing. In *Computer Vision–ECCV 2020: 16th European Conference, Glasgow, UK, August 23–28, 2020, Proceedings, Part I 16*, pages 775–793. Springer, 2020. 3

[32] Xiaofei Li, Jiaxin Yang, Shuohao Li, Jun Lei, Jun Zhang, and Dong Chen. Locate, refine and restore: A progressive enhancement network for camouflaged object detection. In *Proceedings of the Thirty-Second International Joint Conference on Artificial Intelligence, IJCAI-23*, pages 1116–1124. International Joint Conferences on Artificial Intelligence Organization, 2023. Main Track. 2, 5, 6

[33] Fangjian Lin, Yizhe Ma, Sitong Wu, Long Yu, and Shengwei Tian. Axwin transformer: A context-aware vision transformer backbone with axial windows. *arXiv preprint arXiv:2305.01280*, 2023. 3

[34] Jiaying Lin, Xin Tan, Ke Xu, Lizhuang Ma, and Rynson WH Lau. Frequency-aware camouflaged object detection. *ACM Transactions on Multimedia Computing, Communications and Applications*, 19(2):1–16, 2023. 2

[35] Tsung-Yi Lin, Piotr Dollár, Ross Girshick, Kaiming He, Bharath Hariharan, and Serge Belongie. Feature pyramid networks for object detection. In *Proceedings of the IEEE conference on computer vision and pattern recognition*, pages 2117–2125, 2017. 3, 8

[36] Jiawei Liu, Jing Zhang, and Nick Barnes. Modeling aleatoric uncertainty for camouflaged object detection. In *Proceedings of the IEEE/CVF Winter Conference on Applications of Computer Vision*, pages 1445–1454, 2022. 2

[37] Yu Liu, Haihang Li, Juan Cheng, and Xun Chen. Mscaf-net: a general framework for camouflaged object detection via learning multi-scale context-aware features. *IEEE Transactions on Circuits and Systems for Video Technology*, 2023. 2

[38] Ze Liu, Yutong Lin, Yue Cao, Han Hu, Yixuan Wei, Zheng Zhang, Stephen Lin, and Baining Guo. Swin transformer: Hierarchical vision transformer using shifted windows. In *Proceedings of the IEEE/CVF International Conference on Computer Vision*, pages 10012–10022, 2021. 2

[39] Zhengyi Liu, Zhili Zhang, Yacheng Tan, and Wei Wu. Boosting camouflaged object detection with dual-task interactive transformer. In *2022 26th International Conference on Pattern Recognition (ICPR)*, pages 140–146. IEEE, 2022. 5, 6

[40] Zhijian Liu, Xinyu Yang, Haotian Tang, Shang Yang, and Song Han. Flatformer: Flattened window attention for efficient point cloud transformer. In *Proceedings of the IEEE/CVF Conference on Computer Vision and Pattern Recognition*, pages 1200–1211, 2023. 3

[41] Jonathan Long, Evan Shelhamer, and Trevor Darrell. Fully convolutional networks for semantic segmentation. In *Proceedings of the IEEE conference on computer vision and pattern recognition*, pages 3431–3440, 2015. 1, 2

[42] Yunqiu Lv, Jing Zhang, Yuchao Dai, Aixuan Li, Bowen Liu, Nick Barnes, and Deng-Ping Fan. Simultaneously localize, segment and rank the camouflaged objects. In *Proceedings of the IEEE/CVF Conference on Computer Vision and Pattern Recognition*, pages 11591–11601, 2021. 2, 4

[43] Yixuan Lyu, Hong Zhang, Yan Li, Hanyang Liu, Yifan Yang, and Ding Yuan. Uedg: Uncertainty-edge dual guided camouflage object detection. *IEEE Transactions on Multimedia*, 2023. 2, 5, 6

[44] Ran Margolin, Lihi Zelnik-Manor, and Ayellet Tal. How to evaluate foreground maps? In *CVPR*, pages 248–255, 2014. 4

[45] Sachin Mehta and Mohammad Rastegari. Mobilevit: lightweight, general-purpose, and mobile-friendly vision transformer. *arXiv preprint arXiv:2110.02178*, 2021. 3

[46] Haiyang Mei, Ge-Peng Ji, Ziqi Wei, Xin Yang, Xiaopeng Wei, and Deng-Ping Fan. Camouflaged object segmentation with distraction mining. In *Proceedings of the IEEE/CVF Conference on Computer Vision and Pattern Recognition*, pages 8772–8781, 2021. 2

[47] Haiyang Mei, Ke Xu, Yunduo Zhou, Yang Wang, Haiyin Piao, Xiaopeng Wei, and Xin Yang. Camouflaged object segmentation with omni perception. *International Journal of Computer Vision*, pages 1–16, 2023. 5, 6

[48] Youwei Pang, Xiaoqi Zhao, Tian-Zhu Xiang, Lihe Zhang, and Huchuan Lu. Zoom in and out: A mixed-scale triplet network for camouflaged object detection. In *Proceedings of the IEEE/CVF Conference on Computer Vision and Pattern Recognition*, pages 2160–2170, 2022. 1, 2, 4, 5, 6

[49] Jingjing Ren, Xiaowei Hu, Lei Zhu, Xuemiao Xu, Yangyang Xu, Weiming Wang, Zijun Deng, and Pheng-Ann Heng. Deep texture-aware features for camouflaged object detection. *IEEE Transactions on Circuits and Systems for Video Technology*, 2021. 2

[50] Pengzhen Ren, Changlin Li, Guangrun Wang, Yun Xiao, Qing Du, Xiaodan Liang, and Xiaojun Chang. Beyond fixation: Dynamic window visual transformer. In *Proceedings of the IEEE/CVF Conference on Computer Vision and Pattern Recognition*, pages 11987–11997, 2022. 3

[51] Karen Simonyan and Andrew Zisserman. Very deep convolutional networks for large-scale image recognition. *arXiv preprint arXiv:1409.1556*, 2014. 2

[52] Ze Song, Xudong Kang, Xiaohui Wei, Haibo Liu, Renwei Dian, and Shutao Li. Fsnet: Focus scanning network for camouflaged object detection. *IEEE Transactions on Image Processing*, 2023. 2

[53] Dongyue Sun, Shiyao Jiang, and Lin Qi. Edge-aware mirror network for camouflaged object detection. In *2023 IEEE International Conference on Multimedia and Expo (ICME)*, pages 2465–2470. IEEE, 2023. 5, 6

[54] Yujia Sun, Shuo Wang, Chenglizhao Chen, and Tian-Zhu Xiang. Boundary-guided camouflaged object detection. *arXiv preprint arXiv:2207.00794*, 2022. 1, 2, 5, 6

[55] Wenhai Wang, Enze Xie, Xiang Li, Deng-Ping Fan, Kaitao Song, Ding Liang, Tong Lu, Ping Luo, and Ling Shao. Pyramid vision transformer: A versatile backbone for dense prediction without convolutions. In *Proceedings of the IEEE/CVF International Conference on Computer Vision*, pages 568–578, 2021. 2, 3, 8

[56] Wenhai Wang, Enze Xie, Xiang Li, Deng-Ping Fan, Kaitao Song, Ding Liang, Tong Lu, Ping Luo, and Ling Shao. Pvt v2: Improved baselines with pyramid vision transformer. *Computational Visual Media*, 8(3):415–424, 2022. 1, 3

[57] Xiaolong Wang, Ross Girshick, Abhinav Gupta, and Kaiming He. Non-local neural networks. In *Proceedings of the IEEE conference on computer vision and pattern recognition*, pages 7794–7803, 2018. 3

[58] Jun Wei, Shuhui Wang, and Qingming Huang. F^3net: Fusion, feedback and focus for salient object detection. In *AAAI*, pages 12321–12328, 2020. 4

[59] Haozhe Xing, Yan Wang, Xujun Wei, Hao Tang, Shuyong Gao, and Wenqiang Zhang. Go closer to see better: Camouflaged object detection via object area amplification and figure-ground conversion. *IEEE Transactions on Circuits and Systems for Video Technology*, 2023. 2

[60] Haotian Yan, Chuang Zhang, and Ming Wu. Lawin transformer: Improving semantic segmentation transformer with multi-scale representations via large window attention. *arXiv preprint arXiv:2201.01615*, 2022. 3

[61] Fan Yang, Qiang Zhai, Xin Li, Rui Huang, Ao Luo, Hong Cheng, and Deng-Ping Fan. Uncertainty-guided transformer reasoning for camouflaged object detection. In *Proceedings of the IEEE/CVF International Conference on Computer Vision*, pages 4146–4155, 2021. 2

[62] Rui Yang, Hailong Ma, Jie Wu, Yansong Tang, Xuefeng Xiao, Min Zheng, and Xiu Li. Scalablevit: Rethinking the context-oriented generalization of vision transformer. In *European Conference on Computer Vision*, pages 480–496. Springer, 2022. 3

[63] Yang Yang and Qiang Zhang. Finding camouflaged objects along the camouflage mechanisms. *IEEE Transactions on Circuits and Systems for Video Technology*, 2023. 2

[64] Yuhui Yuan, Rao Fu, Lang Huang, Weihong Lin, Chao Zhang, Xilin Chen, and Jingdong Wang. Hrformer: High-resolution vision transformer for dense predict. *Advances in Neural Information Processing Systems*, 34:7281–7293, 2021. 3

[65] Guanghui Yue, Houlu Xiao, Hai Xie, Tianwei Zhou, Wei Zhou, Weiqing Yan, Baoquan Zhao, Tianfu Wang, and Qiuping Jiang. Dual-constraint coarse-to-fine network for camouflaged object detection. *IEEE Transactions on Circuits and Systems for Video Technology*, 2023. 2

[66] Wei Zhai, Yang Cao, HaiYong Xie, and Zheng-Jun Zha. Deep texton-coherence network for camouflaged object detection. *IEEE Transactions on Multimedia*, 2022. 2

[67] Miao Zhang, Shuang Xu, Yongri Piao, Dongxiang Shi, Shusen Lin, and Huchuan Lu. Preynet: Preying on camouflaged objects. In *Proceedings of the 30th ACM International Conference on Multimedia*, pages 5323–5332, 2022. 2

[68] Qiming Zhang, Yufei Xu, Jing Zhang, and Dacheng Tao. Vsa: Learning varied-size window attention in vision transformers. In *European conference on computer vision*, pages 466–483. Springer, 2022. 3

[69] Yi Zhang, Jing Zhang, Wassim Hamidouche, and Olivier Deforges. Predictive uncertainty estimation for camouflaged object detection. *IEEE Transactions on Image Processing*, 2023. 2

[70] Zhemin Zhang and Xun Gong. Axially expanded windows for local-global interaction in vision transformers. *arXiv preprint arXiv:2209.08726*, 2022. 3

[71] Wenda Zhao, Shigeng Xie, Fan Zhao, You He, and Huchuan Lu. Nowhere to disguise: Spot camouflaged objects via saliency attribute transfer. *IEEE Transactions on Image Processing*, 2023. 2

[72] Dehua Zheng, Xiaochen Zheng, Laurence T Yang, Yuan Gao, Chenlu Zhu, and Yiheng Ruan. Mffn: Multi-view feature fusion network for camouflaged object detection. In *Proceedings of the IEEE/CVF Winter Conference on Applications of Computer Vision*, pages 6232–6242, 2023. 2

[73] Zhuo Zheng, Yanfei Zhong, Junjue Wang, Ailong Ma, and Liangpei Zhang. Farseg++: Foreground-aware relation network for geospatial object segmentation in high spatial resolution remote sensing imagery. *IEEE Transactions on Pattern Analysis and Machine Intelligence*, 2023. 3, 8

[74] Yijie Zhong, Bo Li, Lv Tang, Senyun Kuang, Shuang Wu, and Shouhong Ding. Detecting camouflaged object in frequency domain. In *Proceedings of the IEEE/CVF Conference on Computer Vision and Pattern Recognition*, pages 4504–4513, 2022. 2, 5, 6

[75] Tao Zhou, Yi Zhou, Chen Gong, Jian Yang, and Yu Zhang. Feature aggregation and propagation network for camouflaged object detection. *IEEE Transactions on Image Processing*, 31:7036–7047, 2022. 2, 5, 6

[76] Hongwei Zhu, Peng Li, Haoran Xie, Xuefeng Yan, Dong Liang, Dapeng Chen, Mingqiang Wei, and Jing Qin. I can find you! boundary-guided separated attention network for camouflaged object detection. In *Proceedings of the AAAI Conference on Artificial Intelligence*, pages 3608–3616, 2022. 1, 2, 5, 6

[77] Jinchao Zhu, Xiaoyu Zhang, Shuo Zhang, and Junnan Liu. Inferring camouflaged objects by texture-aware interactive guidance network. In *Proceedings of the AAAI Conference on Artificial Intelligence*, pages 3599–3607, 2021. 2